Deteriorated hardened cement paste structure analyzed by XPS and ^{29}Si NMR techniques

Kiyofumi Kurumisawa[1]*, Toyoharu Nawa[2], Hitoshi Owada[3], and Masahito Shibata[4]

*[1]*Faculty of engineering, Hokkaido University, Japan*

Kita 13, Nishi 8, Kita-ku, Sapporo, Hokkaido, 060-8628, Tel:+81-11-706-6319

e-mail:*kurumi@eng.hokudai.ac.jp*

[2]*Faculty of engineering, Hokkaido University, Japan*

Kita 13, Nishi 8, Kita-ku, Sapporo, Hokkaido, 060-8628, Tel:+81-11-706-7274

[3] *Radioactive Waste Management Funding and Research Center, 1-15-7 Tsukishima, Chuo-ku, Tokyo, Japan, Tel+81(3) 3534-4537*

[4] *Taiheiyo Consultant Co.,Ltd., 2-4-2, Ohsaku, Sakura-city, Chiba, Japan, Tel:+81(43)498-3858*

Abstract

In this report, X-ray photoelectron spectroscopy (XPS) and ^{29}Si-MAS-NMR was used for the evaluation of deteriorated hardened cement pastes. The deterioration by ammonium

nitrate solution was accompanied by changes in the pore structure as well as by structural changes in the C-S-H in the hardened cement paste. The CaO/SiO_2 ratio of the C-S-H decreased with the progress of deterioration, there was also polymerization of the silicate in the C-S-H. It was confirmed that the degree of polymerization of silicate of the C-S-H in hardened cement paste can be determined by XPS. It was also shown that the polymerization depends on the structure of the C-S-H.

Keywords: Calcium-Silicate-Hydrate (C-S-H)(B); Degradation(C); ^{29}Si NMR; X-ray photoelectron spectroscopy; CaO/SiO_2 ratio

1. Introduction

When concrete structures are exposed to actual environments for long periods of time, the concrete deteriorates, and the mechanical characteristic of the concrete changes. For example, the storage of radioactive waste is necessary for tens of thousands of years, and the performance of the concrete structures holding it must be maintained during this length of period. It is possible to know the early performance of concrete structures, but it is difficult to know the long-term performance. Therefore, it is very important to know and able to predict the long-term behavior of concrete, and it is important to clarify the mechanisms affecting the behavior. The calcium ion concentration in the pore solution of concrete decreases during long periods, and this leads to a dissolution of the calcium bound in the skeleton of the portlandite crystals $Ca(OH)_2$ and calcium-silica-hydrates (C-S-H). Calcium leaching leads to significant changes in the concrete microstructure, especially, there is a large increase in porosity. Much study focusing on the pore structure has been reported, but there are not many investigations focusing on the calcium silicate hydrate (C-S-H) structure in hardened cement paste, the matrix of the concrete [1-7]. The C-S-H is the main component comprising 60% or more by volume of hardened cement paste, and it controls the properties of hardened cement paste such as the diffusivity and strength [8-10]. The porosity of concrete

changes when concrete is exposed to the elements, and it may be expected that the chemical structure of the C-S-H changes.

Solid-state Nuclear Magnetic Resonance (NMR) and TMS methods have been used for the characterization of silicate anion structures in cement chemistry [11-18]. The NMR measurements are used for bulk measurements. The CaO/SiO_2 ratio and bonding state of the Si in C-S-H is determined by X-ray Photoelectron Spectroscopy (XPS) [19-28]. The differences in polymerization of silica were determined by the binding energy shifts [29-31], highly polymerized silica has higher binding energies. Further, with XPS it is possible to obtain details of the hardened cement paste such as the distribution of Si.

There are some studies of the dissolution of metal from leached cement paste [32,33], but there is no study of the bonding state of silicate in leached cement paste by XPS as far as we know. Therefore this study focuses on changes in the chemical structure of the C-S-H. The purpose of the study is to clarify the effect of leaching on the bonding state of silicate of C-S-H in hardened cement paste by XPS and NMR.

2. Experimental

2.1 Sample preparation.

Ordinary Portland cement (OPC) produced in Japan was used. The density of OPC is

3170kg/m^3 and the blaine surface area of OPC is 3340cm^2/g. The chemical composition and the mineral composition calculated by Bogue equation of OPC is shown in Table 1. The water/cement ratio for the hardened cement pastes (HCP) was 0.6 [34], because of avoiding the effect of unhydrated cement on experimental results. After mixing the specimens were demolded after 24 h, and cured at 50 °C in saturated calcium hydroxide solution for 91days for accelerating the hydration of cement. Ammonium nitrate solution was used to accelerate the deterioration of the hardened cement paste, and the degree of deterioration of the hardened cement paste was simulated by changing the concentration of ammonium nitrate solution [35,36]. It was possible to produce hardened cement pastes with different CaO/SiO_2 ratios by varying the concentration of the ammonium nitrate solutions. In this study, the concentrations of the ammonium nitrate solutions (specimen weight: NH_4NO_3 solution weight=1:30) were 0.25, 0.4, and 0.6M and the immersion time 7days without renewal of solution. The specimen was cut from the center of bulk sample (30mm in diameter and 100mm in height) and the shape of specimens for the immersion was 3mm high and 30mm in diameter to produce homogeneous deterioration of the specimens. After immersion, we measured the CaO/SiO_2 ratios of the cross-section of specimens by EPMA, and confirmed that the samples were homogeneous.

2.2 X-ray diffraction (XRD) measurements.

Samples for the measurements were powder that was crushed by ball mill, dried under Argon gas atmosphere, and mixed with 10%wt of corundum (Al_2O_3) as an internal standard. The conditions of the XRD measurements were 40kV, 40mA, and with an CuKα X-ray monochromater. A 0.02 2θ step and 2-second count time from 5 to 60 degrees was used. The Rietveld method was used for the quantitative analysis of the composition of the hydrated cement (C_3S, C_2S, C_3A, C_4AF, AFm (Monosulfate:$C_3A.CaSO_4.12H_2O$), Aft (Ettringite), CH, Katoite, Gypsum, and Calcite) with the Siroquant software [37].

2.3 Backscattered electron image (BEI) measurements.

A 3 mm cube was cut from freeze dried samples of the hardened cement pastes and used for the BEI observations. These dried specimens were immersed in epoxy resin in vacuum; after the hardening of the epoxy resin, a specimen surface was polished using SiC paper, and finally smoothed by 0.25 micrometer diamond paste, and a carbon coat was applied to provide electric conductivity on the specimen surface. The electron microscopy imaging (Shimadzu, SSX550) was conducted under the following conditions: an acceleration voltage of 15 keV, a working distance of 17 mm, a field size of 200 × 150 μm, and a pixel size of 0.32 μm. The resulting resolution in this study is 0.32 μm, and it

was not possible to distinguish pores narrower than 0.32 μm in diameter. Observations were carried out on 16 fields in each specimen. Unhydrated cement (UH), calcium hydroxide (CH), C-S-H (including fine pores and other hydrates), and pores larger than 0.32 μm were distinguished using image analysis software and setting brightness thresholds. Energy dispersive X-ray analysis (EDX) was used for the determination of CaO/SiO_2 molar ratios (C/S) of the C-S-H distinguished by backscattered electron image.

2.4 Mercury intrusion porosimetry (MIP).

Crushed samples (size: around 3.0mm) that were freeze dried and used for the MIP (AutoPore9500, Micromeritics). The porosity and pore size distribution study was carried out with a mercury intrusion porosimeter capable of generating pressures in the range of subambient to 33,000 psi (227 MPa). The pore radius calculations were done by using the Washburn equation.

2.5 BET surface area measurements.

The BET surface areas of the hydrated cement paste were measured with water a vapor isotherm (Hydrosorb1000, Quantachrome). Samples used in the measurements were powder that was crushed with a ball mill and dried by freeze-drying. The samples were placed in a vacuumed desiccator at 105 degree Celsius for 1hour before the

measurements, and the range of the measurements was at 0.05-0.98 in relative pressure. The surface area was determined from an adsorption curve by the multi point BET method.

2.6 NMR measurements.

Measurement of the ^{29}Si-NMR(MAS) spectra was performed at a frequency of 79.49MHz, delayed time of 30 seconds, 7.0mm probe, spinning speed of approximately 4kHz, and number of scanning points is 2000 (MSL 400, Bruker). When the ^{29}Si nuclei are subjected to the NMR, the silicate anions (SiO_4^{4-}) in a calcium silicate component shows Q^0 to Q^4 peaks in the spectrum representing the chain structures. In C-S-H, the major constituent of HCP, the Q^1 (chain end) and Q^2 (within chain) are the major chain structures and neither Q^3 (branching chain) nor Q^4 (networked chain) can be observed. It is also known that the spectrum of the silicate anion is represented in the range of −65 to −78 ppm for Q^0, −78.0 for Q^1, −81.0 for Q^{2Al}, −82.8 for Q^{2p}, −83.4 for Q^{2i}, −85.3 for Q^{2Ca}, −93 to −102 for Q^3, and −107 to −115ppm for Q^4[38,39]. The deconvolution of each silicate anion was analyzed with Lorentzian function by Nuts software (Acorn NMR inc). The mean chain length (MCL) or number of SiO_4 tetrahedra in C-S-H can be calculated from Richardson's equation [16],

$$MCL = \frac{2 \times (Q1 + Q2)}{Q1} \qquad (1)$$

2.7 XPS measurements.

A plate sample (5*5*1mm) that was polished was used for the XPS measurements. Analysis was performed using a JEOL JPS-9200 fitted with a Mg K_α (hv=1253.6eV) X-ray source operating at 100 W (10 kV, 10 mA). The area for the XPS analysis was 3mm in diameter with a high vacuum condition ($<10^{-6}$Pa). The spectra were corrected for charging effects using the adventitious hydrocarbon peak at 284.8 eV binding energy. Deconvolution of spectrum was analyzed by Specsurf software (JEOL).

3. Results and discussion

Fig.1 shows backscattered electron images of HCP; the black, dark grey, and light grey show pore, C-S-H, and CH, respectively, and the white pixels show unhydrated cement (UH). Large pores (>0.32μm) increased with increases in the NH_4NO_3 concentration of the immersion solution. White portions still remained in the deteriorated specimen, this contained Fe. Therefore, it is considered that unhydrated cement such as C_4AF.

XRD patterns of specimens were shown in Fig.2, and Table 2 shows the results of the mineral compositions determinations of the HCP specimens measured by the XRD Rietveld method, and the CaO/SiO_2 molar ratios of the C-S-H measured by EDX. The XRD results show that the calcium hydroxide and aluminate hydrates in the

deteriorated specimens with the NH_4NO_3 addition was not detected by XRD, as in previous reports [6,40,41]. The C/S of the C-S-H decreased with the increases in NH_4NO_3 concentration in the immersion solution, showing that it is possible to produce specimens with different C/S by adjusting the concentration of the NH_4NO_3 solution.

Fig.3 plots the pore size distribution of the specimens measured by MIP. The porosity of the hardened cement paste increased with increases in the concentration of the ammonium nitrate solution. The threshold value of pore diameters is 0.1 μm in non-deteriorated specimens, while it is about 1 μm in the deteriorated specimens, showing that the deteriorated specimens have a coarser structure. This result is the same tendency of previous report [41,42], it was approximately 1.0 and 2.5μm to exposure of NH_4NO_3 solution, and threshold pore diameter increase with the progress of deterioration. The BET surface areas determined by H_2O adsorption is shown in Table 2. The BET surface area of the hardened cement paste increased with the increases in the concentration of ammonium nitrate solution except in the 0.25M specimens.

Fig.4 shows the ^{29}Si-NMR spectrums of the specimens, and the deconvolution of ^{29}Si-NMR spectrums of non-deteriorated specimens was shown in Fig.5 for example, and the fractions of the chemical states of silicate anions in HCP are shown in Fig.6. The ^{29}Si-NMR results indicate that Q^2 increased with the increases in the solution

concentration, and that Q^1 decreased with the increases in the solution concentration, showing that the polymerization of silicate in deteriorated specimens increases. The spectrum of Q^3 that is not detected in non-deteriorated specimens appeared at C/S 0.8. However, there is no Q^3 spectrum of synthesized C-S-H that is produced without hydrothermal treatment in previous reports [17,43]. This suggests that the chemical bonding states of Si in the deteriorated and synthesized C-S-H are different. The calculated mean chain lengths of non-deteriorated, 0.25M, 0.4M and 0.6M NH_4NO_3 treated specimens from the NMR results were 4.6, 6.6, 7.1, and 14.3 respectively. The chain length of the C/S 0.8 specimen is 3 times longer than that of non-deteriorated specimen, suggesting the progress of polymerization. The mean chain length of C/S 1.8 and C/S 0.7 is 3.2 and 18.6 respectively by previous report [44]. It is also reported that Q2/Q1 ratio increase with the progress of leaching [5], the progress of polymerization of silicate by calcium leaching is reported by previous reports [45,46]. Fig.7 plots $Q^1/\sum Q^i$ versus the C/S ratio for C-S-H, the values determined in this study and for 1.4nm Tobermorite and Jennite reported in a previous study [15]. When it is the same crystal structure, it is plotted on the same straight line. This suggests that the structure of the C-S-H immersed in 0.4 and 0.6M NH_4NO_3 is similar to the crystal structure of tobermorite and the C-S-H in the previous study [15], the specimens immersed in 0.25M

NH_4NO_3 and the non-deteriorated specimens are similar to the crystal structure of jennite. It is considered that the structure of the C-S-H varied due to the differences in the NH_4NO_3 concentration of the immersion solutions.

Fig.8 shows the photoelectron spectra of HCP measured by XPS. From results of the XPS, the peak heights of calcium decreased, and those of the silica increased with the degree of deterioration. Fig.9 and 10 show the Ca 2p and Si 2p spectra of the non-deteriorated and deteriorated specimens. Although the relative intensity of Ca 2p decreased with the decreases in C/S, the peak value of binding energy of Ca 2p in non-deteriorated specimen measured by XPS is not different from that in deteriorated specimens. However, the binding energy of Si 2p was shifted, and increased with the increases in the concentration in NH_4NO_3 immersion solution, this may show that Si is chemically combined with oxide. The difference in the binding energies in Si 2p between C/S 1.8 and 0.8 is more than 1.0eV. The deconvolution of photoelectron spectra (Si2p) of 0.6M NH_4NO_3 specimen is shown in Fig.11. There are two components such as high (102 eV) and low (100.5eV) binding energy. It was shown that the silicate chain length in the deteriorated specimens that were immersed in ammonium nitrate solution is longer than that in the non-deteriorated specimens. This result is in good agreement with the results determined by ^{29}Si-NMR, and clearly suggests that it is possible to determine

the polymerization of silicate in C-S-H by XPS like in the measurements of NMR. Fig.12 shows the relationship between CaO/SiO_2 and the Si 2p binding energies of C-S-H plotted together with the results of previous reports [19, 28]. Here the binding energies of the C-S-H immersed in 0.4 and 0.6M NH_4NO_3 are close to those in the previous studies. However, the binding energies of C-S-H immersed in 0.25M and non-deteriorated specimens are different from those in the previous reports. Here it may be hypothesized that the effect of the binding energy in the unhydrated cement is included in the results, and that the structure of the C-S-H is different as suggested in Fig.7. Overall, this would suggest that the structure of the C-S-H in the deteriorated specimens may be similar to that of the synthetic C-S-H.

4. Conclusions

X-ray photoelectron spectroscopy and ^{29}Si-NMR was used for the evaluation of deteriorated hardened cement pastes. The deterioration by ammonium nitrate solution was accompanied by changes in the pore structure as well as structural changes in the C-S-H of hardened cement paste. The CaO/SiO_2 ratio decreased with the progress of the deterioration, and there was polymerization of silicate in the C-S-H. The degree of polymerization of silicate of the C-S-H in the hardened cement paste can be observed by

XPS. It was shown that the degree of the polymerization of silicate of the C-S-H depends on the structure of C-S-H. Therefore, it is suggested that the structure of the C-S-H in the deteriorated specimens may be similar to that of the synthetic C-S-H.

Acknowledgments

This research includes a part of the results of "Evaluation Experiments of Long-Term Performance of Engineered Barriers, FY2012" under a grant from the Agency for Natural Resources and energy in the Ministry of Economy, Trade and Industry (METI) of Japan. We thank the Ministry of Education, Culture, Sports, Science and Technology for the financial support with the research here. And we also thank Mr. Suzuki and Mr. Kurosawa of Hokkaido University for help with the measurements.

References

[1] P.Faucon et.al., Long-term behavior of cement pastes used for nuclear waste disposal: review of physic-chemical mechanisms of water degradation, Cem. Concr. Res., 28(1998)847-857

[2] Adenot F, Buil M., Modelling of the corrosion of the cement paste by deionized water, Cem. Concr. Res., 22(1992) 489–96

[3] C. Carde, R. Francois, J.M. Torrenti, Leaching of both calcium hydrate and C-S-H from paste: modeling the mechanical behavior, Cem. Concr. Res., 26 (1996) 1257-1268

[4] Heukamp FH, Ulm FJ, Germaine JT., Mechanical properties of calcium-leached cement pastes Triaxial stress states and the influences of the pore pressures. Cem Concr Res.,31(2001)767–774

[5] K. Haga, M. Shibata, M. Hironaga, S. Tanaka, S. Nagasaki, Silicate anion structural change in calcium silicate hydrate gel on dissolution of hydrated cement, J. Nucl. Sci. 5 (2002) 540–547

[6] C. Carde, G. Escadeillas, A. H. François, Use of ammonium nitrate solution to simulate and accelerate the leaching of cement pastes due to deionized water, Mag.Concr. Res., 49(1997) 295 –301

[7] Siham Kamali, Micheline Moranville, Stéphanie Leclercq, Material and environmental parameter effects on the leaching of cement pastes: Experiments and modelling, Cem.Concr. Res., 38(2008) 575-585

[8] R.F. Feldman, J.J. Beaudoin, Microstructure and strength of hydrated cement, Cem. Conc. Res., 6(1976)389-400

[9] Georgios Constantinides, Franz-Josef Ulm, The effect of two types of C-S-H on the elasticity of cement-based materials: Results from nanoindentation and micromechanical modeling, Cem. Concr. Res., 34(2004) 67-80

[10] Kiyofumi Kurumisawa, Toyoharu Nawa, Hitoshi Owada, Prediction of the diffusivity of cement-based materials using a three-dimensional spatial distribution model, Cem. Concr. Comp.,34(2012)408-418

[11] I.G.Richardson, The nature of C-S-H in hardened cements, Cem.Concr.Res., 29(1999) 1131-1147

[12] H.F.W. Taylor, Proposed structure for calcium silicate hydrate gel, J. Am. Ceram. Soc.69 (1986) 464–467

[13] H.F.W. Taylor, Tobermorite, jennite, and cement gel, Z. Kristallogr. 202 (1992)41–50.

[14] K. Fujii, W. Kondo, Estimation of thermochemical data for calcium silicate hydrate(C-S-H), J. Am. Ceram. Soc., 66 (1983) 220–221.

[15] X.D. Cong, R.J. Kirkpatrick, 29MAS NMR study of the structure of calcium silicate hydrate, Adv. Cem. Based Mater., 3 (1996) 144–156.

[16] I.G. Richardson, Tobermorite/jennite- and tobermorite/calcium hydroxide-based models for the structure of C-S-H: applicability to hardened pastes of tricalciumsilicate,

ß-dicalcium silicate, Portland cement, and blends of Portland cement with blast-furnace slag, metakaolin, or silica fume, Cem. Concr. Res., 34 (2004)1733–1777.

[17] H.Viallis, P.Faucon, J.-C.Petit and A.Nonat, Interaction between Salts (NaCl, CsCl) and Calcium Silicate Hydrates (C-S-H), J.Phys. Chem. B, 103(1999) 5212-5219

[18] L. Zhang, Z. Li, Z. Lin, The structure of silicate ions in C-S-H discussed from chemical composition, Adv. Cem. Res., 24(2012)263-281

[19] Leon Black, Andreas Stumm, Krassimir Garbev, Peter Stemmermann, Keith R.Hallam, Geoffrey C. Allen, X-ray photoelectron spectroscopy of the cement clinker phases tricalcium silicate and ß-dicalcium silicate, Cem. Concr. Res., 33 (2003) 1561–1565.

[20] M. Regourd, J.H. Thomassin, P. Baillif, J.C. Touray, Study of the early hydration of Ca3SiO5 by X-ray photoelectron spectrometry, Cem. Concr. Res., 10 (1980) 223–230.

[21] D. Ménétrier, I. Jawed, T.S. Sun, J. Skalny, ESCA and SEM studies on early C3S hydration, Cem. Concr. Res., 9 (1979) 473–482

[22] A. Stumm, K. Garbev, G. Beuchle, L. Black, P. Stemmermann, R. Nüesch, Formation of C-S-H (I) and its hydrothermal analogue gyrolite in the system CaO-ZnO-SiO2-H2O, Cem. Concr. Res., 35 (2005) 1665–1675.

[23] L. Black, A. Stumm, K. Garbev, P. Stemmermann, K.R. Hallam, G.C. Allen, X-ray photoelectron spectroscopy of aluminium-substituted tobermorite, Cem. Concr.Res., 35(2005) 51–55.

[24] L. Black, K. Garbev, P. Stemmermann, K.R. Hallam, G.C. Allen, Characterisation of crystalline C-S-H phases by X-ray Photoelectron Spectroscopy (XPS), Cem. Concr. Res., 33 (2003) 899–911.

[25] L. Black, K. Garbev, P. Stemmermann, K.R. Hallam, G.C. Allen, Erratum to“characterisation of crystalline C-S-H phases by X-ray Photoelectron Spectroscopy(XPS), Cem. Concr. Res., vol 33 (2003), pp.899–911, Cem. Concr. Res., 33 (2003) 1913.

[26] L. Black, K. Garbev, G. Beuchle, P. Stemmermann, D. Schild, X-ray photoelectron spectroscopic investigation of nanocrystalline calcium silicate hydrates synthesised by reactive milling, Cem. Concr. Res., 36 (2006) 1023–1031

[27] L. Black, K. Garbev, P. Stemmermann, K.R. Hallam, G.C. Allen, X-ray Photoelectron Study of oxygen bonding in crystalline C-S-H phases, Phys. Chem. Miner., 31 (2004) 337–346.

[28] L. Black, K. Garbev, and I. Gee, A Comparison between Fresh and Aged C–S–H Using X-ray Photoelectron Spectroscopy, Cem. Concr. Res., 38(2008) 745–50.

[29] K. Okada, Y. Kameshima, A. Yasumori, Chemical shifts of silicon X-ray photoelectron spectra by polymerization structures of silicates, J. Am. Ceram. Soc., 81 (1998) 1970–1972.

[30] H. Seyama, M. Soma, Bonding-state characterization of the constituent elements of silicate minerals by X-ray photoelectron spectroscopy, J. Chem. Soc. Faraday Trans.,81 (1985) 485–495.

[31] Hawthorne (Ed.), Spectroscopic Methods in Mineralogy and Geology, Reviews in Mineralogy, Mineralogical Society of America, 18 (1988) 573–637.

[32] David L. Cocke, M.Yousuf A. Mollah, J.R. Parga, Thomas R. Hess, J.Dale Ortego, An XPS and SEM/EDS characterization of leaching effects on lead- and zinc-doped portland cement, J. Hazard. Mater., 30(1992) 83-95

[33] Ghaleb N Salaita, Philip H Tate, Spectroscopic and microscopic characterization of portland cement based unleached and leached solidified waste, Appl. Surf. Sci.,133(1998) 33-46

[34] H24 Report of Project for Evaluation on the long-term performance of engineered barrier system. Radioactive Waste Management Funding and Research Center, 2013

[35] C. Carde, R. Francois, Effect of the leaching of calcium hydroxide from cement paste on mechanical and physical properties, Cem. Concr. Res., 27(1997) 539–550

[36] Micheline Moranville, Siham Kamali, Emmanuel Guillon, Physicochemical equilibria of cement-based materials in aggressive environments—experiment and modeling, Cem.Concr. Res., 34(2004) 1569-1578

[37] Pipat Termkhajornkit, Toyoharu Nawa, Kiyofumi Kurumisawa, Effect of water curing conditions on the hydration degree and compressive strengths of fly ash–cement paste, Cem. Conc. Comp., 28(2006) 781-789

[38] Fumiaki Matsushita, Yoshimichi Aono, Sumio Shibata, Calcium silicate structure and carbonation shrinkage of a tobermorite-based material, Cem.Conc.Res., 34(2004) 1251-1257

[39] Morten Daugaard Andersen, Hans J. Jakobsen, Jørgen Skibsted, Characterization of white Portland cement hydration and the C-S-H structure in the presence of sodium aluminate by 27Al and 29Si MAS NMR spectroscopy, Cem.Conc.Res., 34(2004) 857-868

[40] P.Faucon et.al., Leaching of cement：study of the surface layer, Ceme. Concr. Res., 26(1996)1707-1715

[41] C. Gallé, H. Peycelon, P. Le Bescop, Effect of an accelerated chemical degradation on water permeability and pore structure of cementbased materials, Adv. Cem. Res., 16(2004) 105 –114

[42] I. Segura, M. Molero, S. Aparicio, J.J. Anaya, A. Moragues, Decalcification of cement mortars: Characterisation and modelling, Cem.Conc.Comp., 35(2013),136-150

[43] Jung J. Kim, Emmy M. Foley, Mahmoud M. Reda Taha, Nano-mechanical characterization of synthetic calcium–silicate–hydrate (C–S–H) with varying CaO/SiO2 mixture ratios, Cem.Conc. Comp., 36(2013) 65-70

[44] Jeffrey J. Chen, Jeffrey J. Thomas, Hal F.W. Taylor, Hamlin M. Jennings, Solubility and structure of calcium silicate hydrate, Cem.Conc.Res., 34(2004) 1499-1519

[45] J.J. Gaitero, I. Campillo, A. Guerrero, Reduction of the calcium leaching rate of cement paste by addition of silica nanoparticles, Cem.Conc.Res., 38(2008) 1112-1118

[46] P. Faucon, F. Adenot, J. Facquinot, J. Virlet, R. Cabrillac, M.Jorda, Contribution of nuclear magnetic resonance techniques to the study of cement paste water degradation, Proc. 10th Int.Congress on the Chemistry of Cement, (1997) 3v003

Tables

Table 1 The chemical composition and mineral composition of cement

Chemical composition (wt%)	
CaO	64.56
SiO2	21.52
Al2O3	5.22
Fe2O3	2.65
MgO	1.45
SO3	2.04
Na2O	0.28
K2O	0.47
TiO2	0.28
P2O5	0.23
MnO	0.09
Cl	0.011
ig.loss	1.13
Mineral composition of the cement by Bogue, calculated (%)	
C3S	62.1
C2S	14.9
C3A	9.4
C4AF	8.1

Table 2 Mineral compositions (wt%) and CaO/SiO2 molar ratios of HCP.

	Non-deteriorated	0.25M NH4NO3	0.4M NH4NO3	0.6M NH4NO3
Unhydrated cement	2.5	5.5	5.1	6.0
CH	19.0	-	-	-
AFm	5.3	0.4	0.7	0.1
AFt	0.1	3.2	1.5	0.7
Katoite	4.4	6.5	8.2	9.7
Amorphous	68.3	82.9	82.2	81.4
CaO/SiO2	1.83	1.62	1.04	0.83

Table 3 BET surface areas of specimens (m^2/g)

Non-deteriorated	0.25M NH_4NO_3	0.4M NH_4NO_3	0.6M NH_4NO_3
221.9	363.1	299.4	362.2

Figure captions

Fig.1 Backscattered electron image of specimens (Size: 200*150μm, a: Non-deteriorated, b: 0.25M NH_4NO_3, c: 0.4M NH_4NO_3, d: 0.6M NH_4NO3)

Fig.2 XRD pattern of specimens

Fig.3 Pore size distributions in specimens

Fig.4 29Si-NMR spectrums of specimens

Fig.5 Deconvolution data of ^{29}Si-NMR spectrums of non-deteriorated specimen

Fig.6 Fraction of chemical bonding of SiO_4^{4-} by NMR

Fig.7 Plot of Q1/∑Qi vs. C/S ratios for C-S-H, 1.4nm tobermorite and Jennite

(a: Non-deteriorated, b: 0.25M NH_4NO_3, c: 0.4M NH_4NO_3, d: 0.6M NH_4NO_3)

Fig.8 Photoelectron spectra (wide range)

Fig.9 Photoelectron spectra (Ca2p)

Fig.10 Photoelectron spectra (Si2p)

Fig.11 Deconvolution of photoelectron spectra (Si2p) of 0.6M NH4NO3 specimen

Fig.12 Plot of CaO/SiO_2 vs. Si 2p binding energy of C-S-H

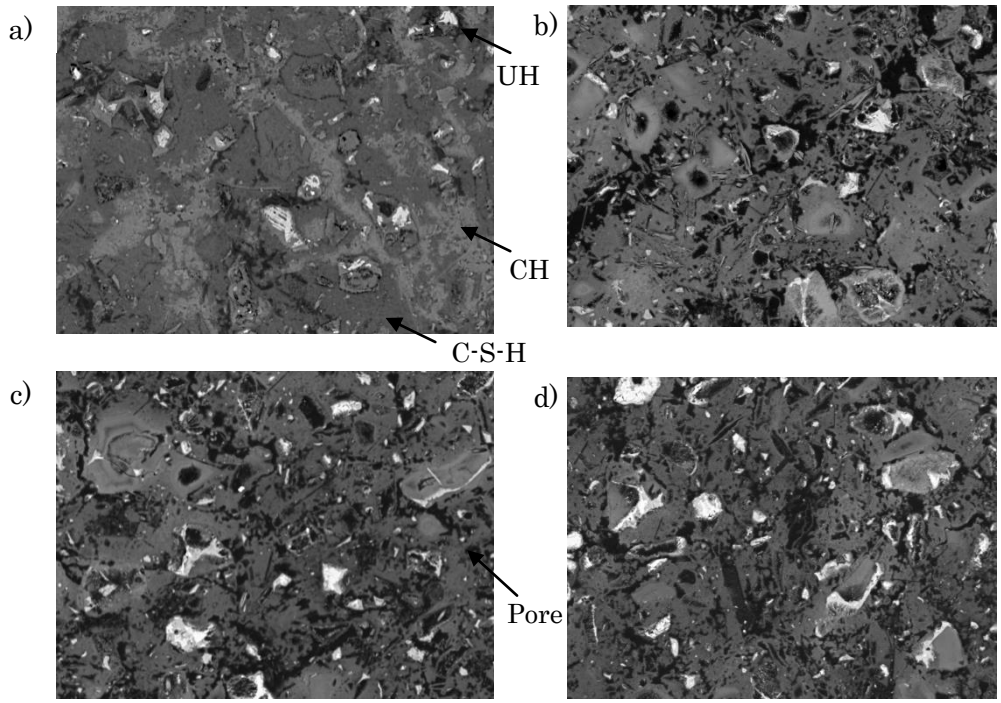

Fig.1 Backscattered electron image of specimens (Size: 200*150μm, a: Non-deteriorated, b: 0.25M NH_4NO_3, c: 0.4M NH_4NO_3, d: 0.6M NH_4NO_3)

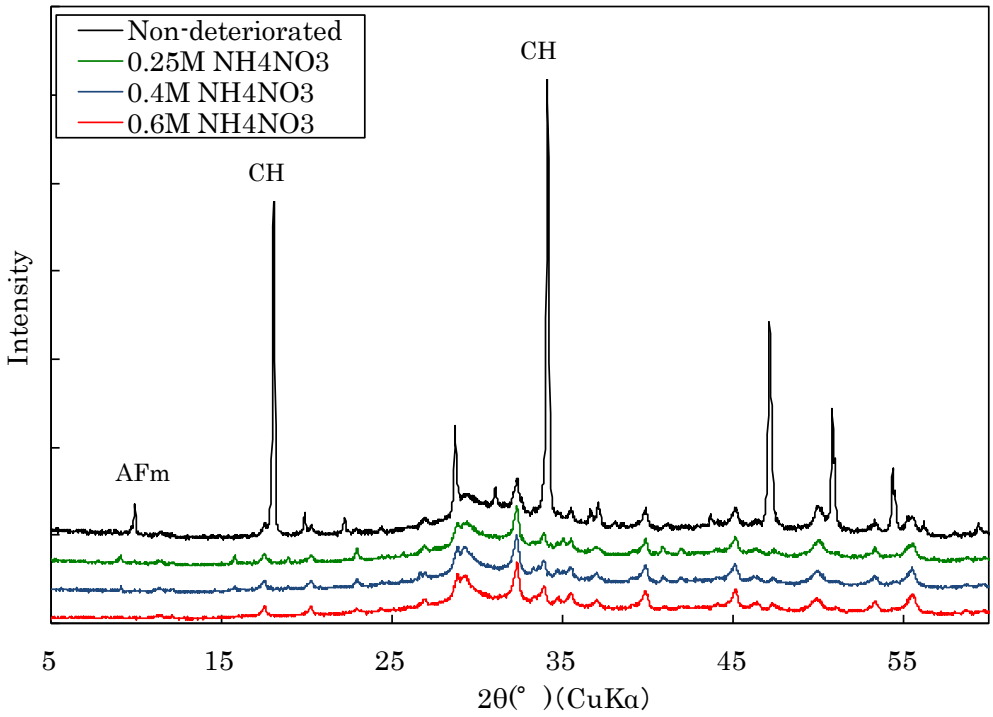

Fig.2 XRD pattern of specimens

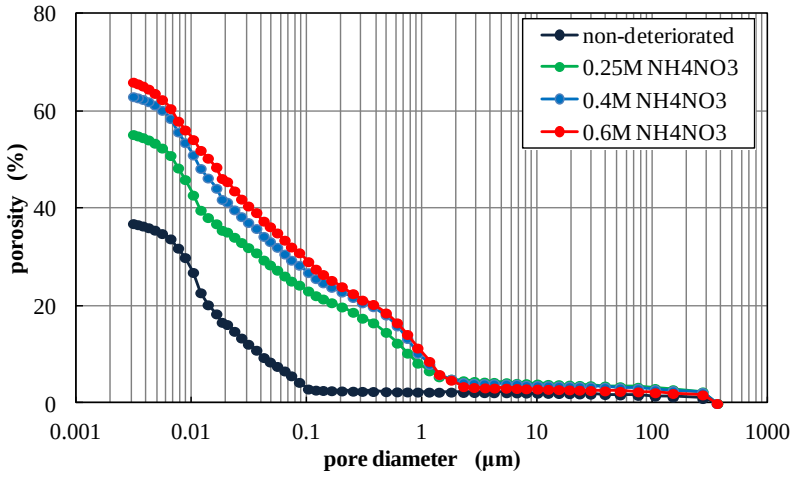

Fig.3 Pore size distributions in specimens

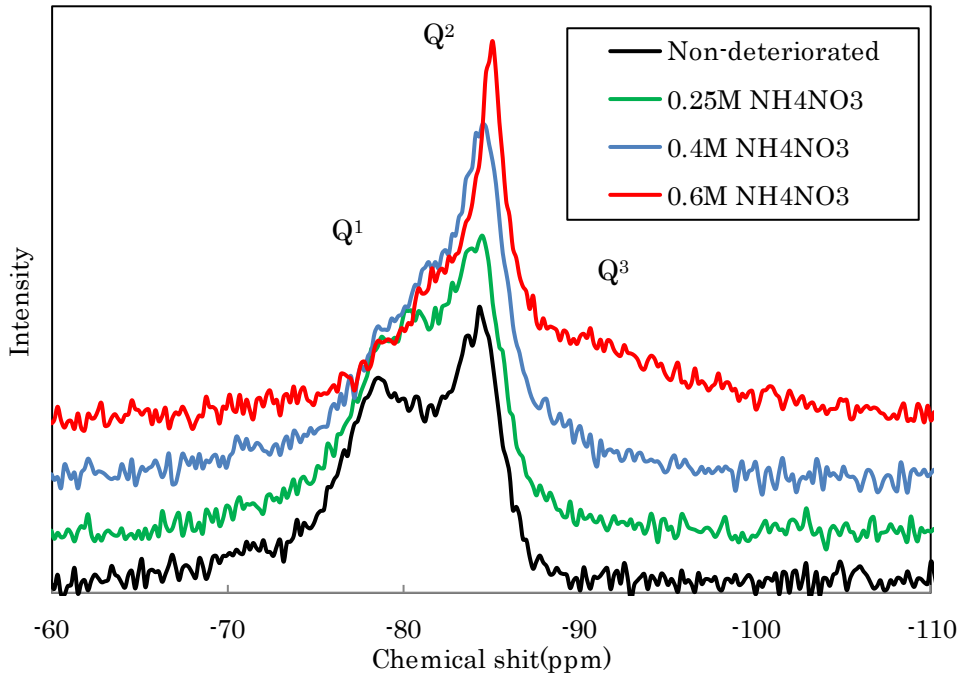

Fig.4 ^{29}Si-NMR spectrums of specimens

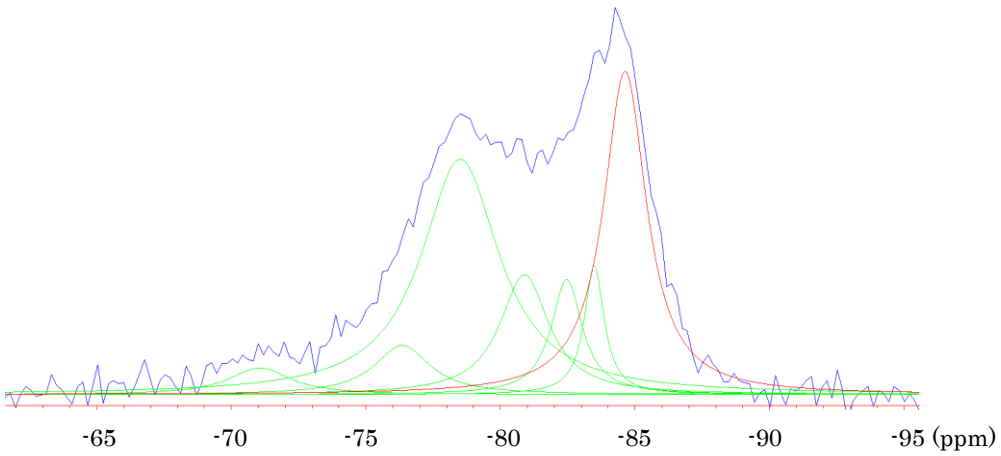

Fig.5 Deconvolution data of ^{29}Si-NMR spectrums of non-deteriorated specimen

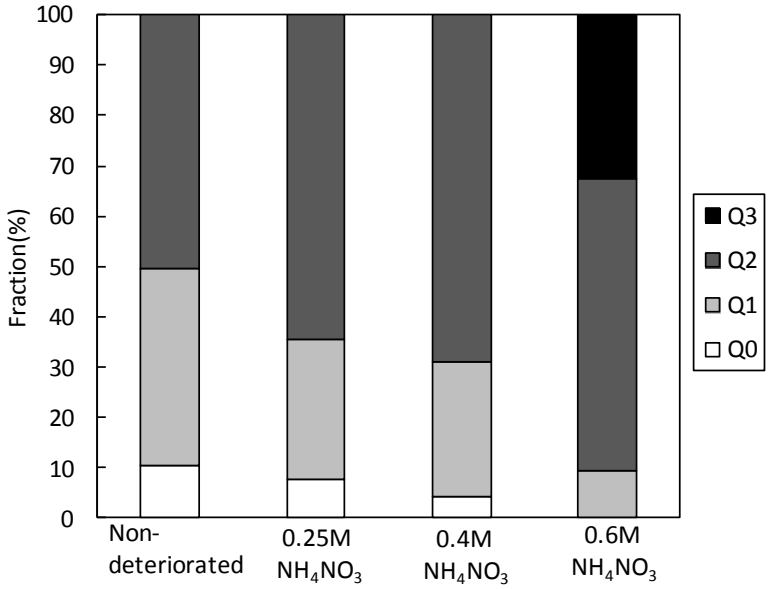

Fig.6　Fraction of chemical bonding of SiO_4^{4-} by NMR

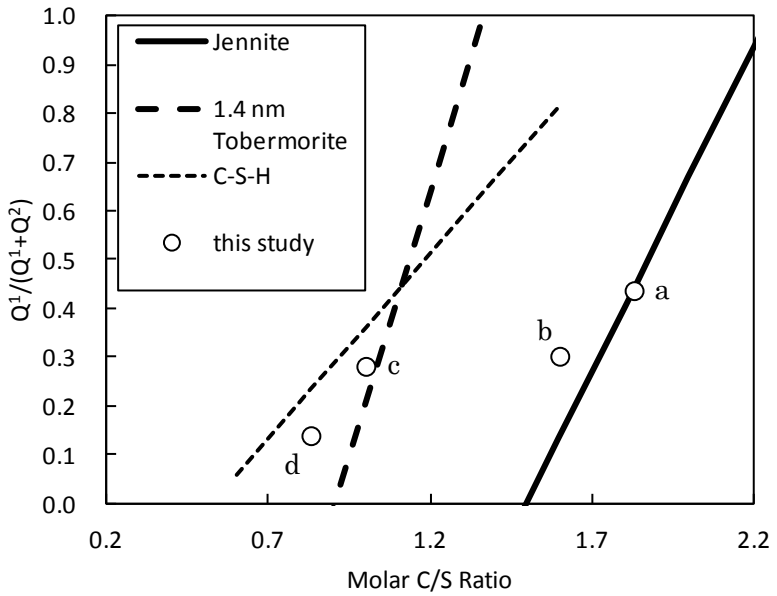

Fig.7 Plot of $Q^1/\sum Q^i$ vs. C/S ratios for C-S-H, 1.4nm tobermorite and Jennite (a: Non-deteriorated, b: 0.25M NH_4NO_3, c: 0.4M NH_4NO_3, d: 0.6M NH_4NO_3)

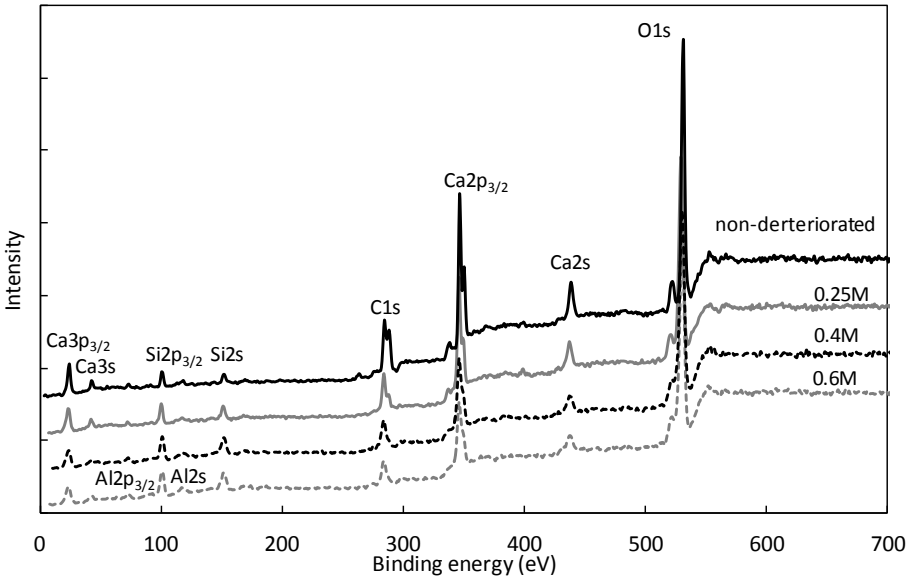

Fig.8 Photoelectron spectra (wide range)

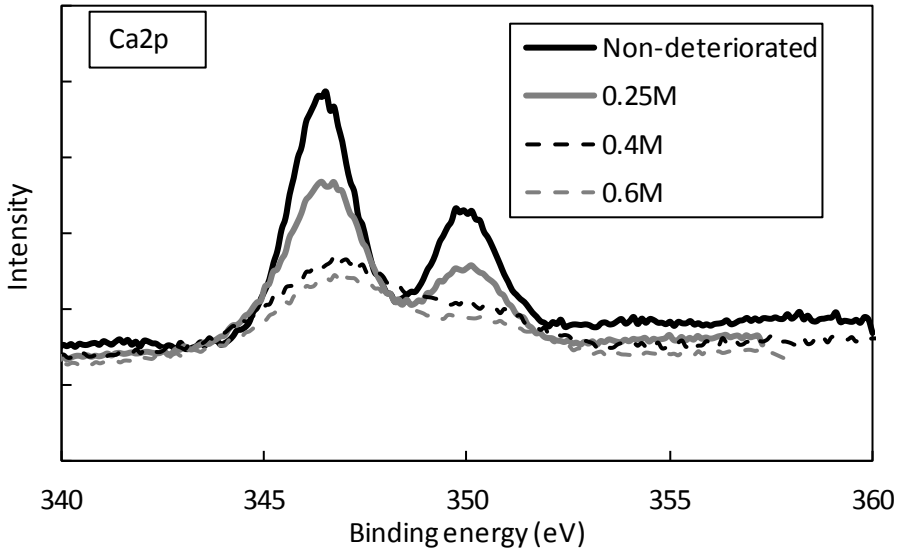

Fig.9 Photoelectron spectra (Ca2p)

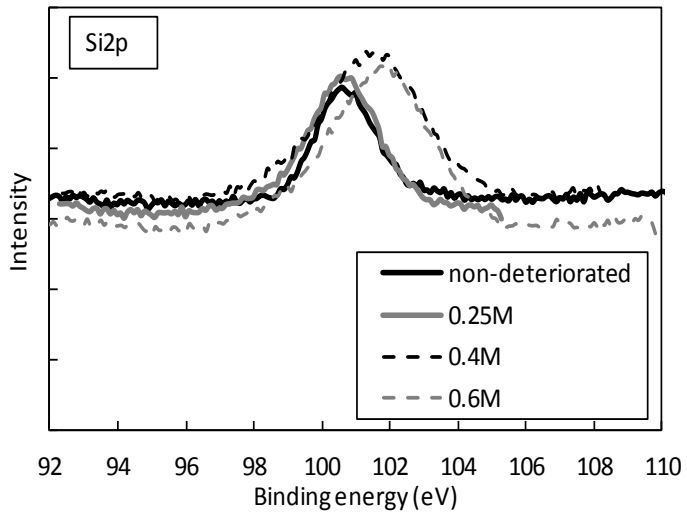

Fig.10 Photoelectron spectra (Si2p)

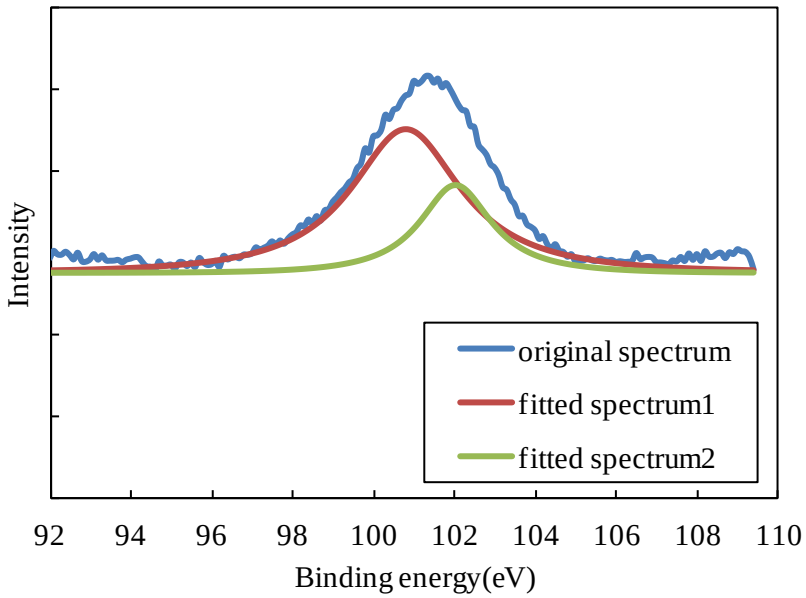

Fig.11 Deconvolution of photoelectron spectra (Si2p) of 0.6M NH_4NO_3 specimen

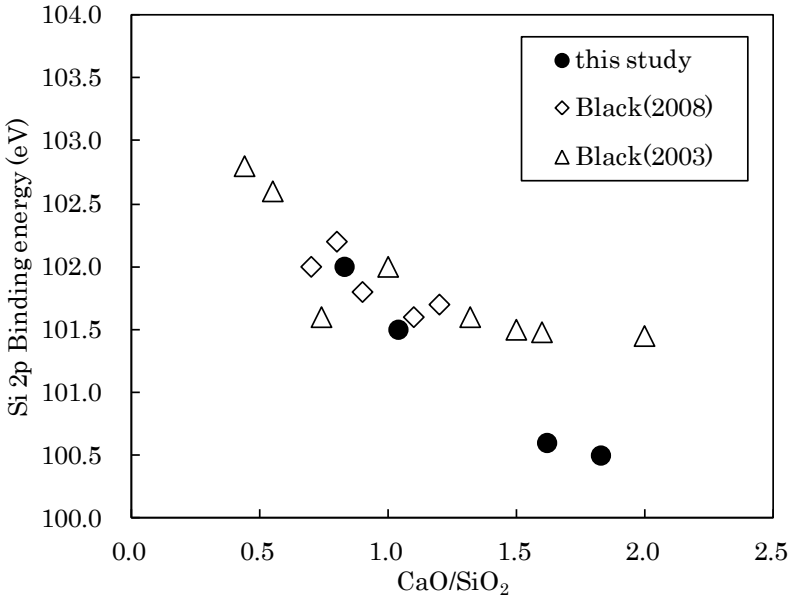

Fig.12 Plot of CaO/SiO_2 vs. Si 2p binding energy of C-S-H

Research highlights

- The degree of polymerization of silicate of the C-S-H in the hardened cement paste can be observed by XPS.
- The structure of C-S-H changed with the degree of calcium leaching.
- The result of NMR about Silicate in C-S-H was in good agreement with the result of XPS.